Autopsy of Nanofiltration membrane of a decentralized demineralization plant

Soufian El-ghzizel[*1], Hicham Jalté[1], Hajar Zeggar[1], Mohamed Zait[1], Sakina Belhamidi[1],
Fathallah Tiyal[1], Mahmoud Hafsi[2], Mohamed Taky[1] and Azzedine Elmidaoui[1]

[1]*Laboratory of Separation Processes, Department of Chemistry, Faculty of Sciences, Ibn Tofail University, Kenitra 14000, Morocco*
[2]*International Institute for Water and Sanitation, National Office of Electricity and potable Water ONEE-IEA, Rabat, Morocco*

Abstract. In 2014, the first demineralization plant, using nanofiltration (NF) membrane coupled with renewable energies was realized at Al Annouar high school of Sidi Taibi, Kenitra, Morocco. This project has revealed difficulties related to the membrane performances loss (pressure increase, flux decline, poor water quality of the produced water and increase of energy consumption), as consequences of membrane fouling. To solve this problem, an autopsy of the membrane was done in order to determine the nature and origin of the fouling. The samples of membrane and fouling were then analyzed by scanning electron microscopy using a scanning electron microscope (SEM) connected with an energy dispersive X-ray (EDX) detection system and X-ray diffractometer (XRD). Moreover, three cleaning solutions (hydrochloric acid, nitric acid and sulfuric acid) were tested and assessed in a single cleaning step to find the suitable one for the fouled membrane to regain its initial permeability and performances. The analysis of the experimental results showed that the fouling layer is mainly composed of calcium carbonate (inorganic fouling). Results showed also that the permeability is improved by the hydrochloric acid cleaning (pH=3) with a cleaning efficiency of 93%. Cleaning efficiency did not exceed 75 % with nitric acid (pH=3) and 40 % with sulfuric acid (pH= 3).

Keywords: nanofiltration; desalination plant; fouling; autopsy; demineralization; membrane cleaning

1. Introduction

Nanofiltration is a promising desalination process that is reported suitable for several applications in many regions in the world, especially in countries suffering water shortage or scarcity. It is denned as a process with special characteristics that cover an intermediate separation range between ultrafiltration and reverse osmosis (Fang *et al*. 2019). Moreover, Nanofiltration is extensively employed to treat all kinds of water such as underground, surface for the production of safe drinking water and wastewater for the recovery of the water industrially reusable (Epsztein *et al*. 2015, Tarek *et al*. 2018). Besides, nanofiltration membrane is increasingly deployed for the removal of solutes ranging from colloidal particles and organic molecules to salts in single unit operation. It is also designed to provide higher water flux at lower pressures than reverse osmosis membranes, and the power requirements are significantly reduced (Pontié *et al*. 2008, Epsztein *et al*. 2018, Jadhav *et al*. 2016). Moreover, NF membranes are the best candidates for water softening as they provide a high rejection of divalent ions (>99%) (Song *et al*. 2016).

Despite the progress made in nanofiltration processes, scaling and fouling are the most serious problems that negatively affect the membrane performances, for instance, poor permeate quality, decrease of flux, increases in operating pressure, energy consumption and treatment cost (Goh *et al*. 2018, Jiang *et al*. 2017, Aguiar *et al*. 2018). This phenomenon is influenced by many factors such as the properties of the membrane material, the feed water constituents and also the operating conditions of the membrane process (Leo *et al*. 2016). Consequently, one or more types of fouling can take place simultaneously such as biofouling, organic fouling and inorganic scaling (Abid *et al*. 2017).

Typically, the membrane fouling characterization can be divided into two different methods, nondestructive and destructive methods (membrane autopsy). Each class of methods has its advantages and disadvantages in identifying the root cause of the fouling. Although nondestructive methods, e.g., quality of the produced water, permeate flux, pressure drop and energy consumption are monitored continuously as a function of filtration time to evaluate the development of fouling during the operation, but these methods are incomplete to determine the principal cause of fouling and its category. For this reason, the membrane has to be destructively diagnosed and autopsied (Destructive methods) to identify the types and quantities of the foulants. Thus, membrane autopsy is recommended to perform at the laboratory level prior to the large scale membrane process implementation (Ruiz-Garcíaa *et al*. 2018).

Membrane autopsy is a destructive method which requires a sacrificial membrane element to be removed from the plant and characterized by using predominantly surface characterization techniques, such as total reflectance Fourier transform infrared (ATR-FTIR), scanning electron microscopy (SEM) or field emission scanning electron microscopy (FESEM), energy dispersive X-ray (EDX)

---

*Corresponding author, Ph.D.
 E-mail: elghzizelsoufian85@gmail.com

spectroscopy, atomic force microscopy (AFM), and X-ray diffractometry (XRD) (Karime *et al*. 2008). The purpose of these techniques is to analyze and identify the foulants in order to develop strategies to minimize fouling phenomenon and improve the long-term efficiency of the membrane, including cleaning membrane methods (physical and/ or chemical cleaning).

Physical cleaning processes are based on five different methods, such as hydraulic (flushing, back pulse and back flush), pneumatic (air sparging, air lifting, air scouring…), mechanic (sponge ball and fluidized particle cleaning), ultrasound irradiation (sonication) and applied electric fields (Regula *et al*. 2014, Lee *et al*. 2010); they are practically performed at regular intervals and specifically employed to eliminate reversible membrane fouling (Kimura *et al*. 2004). Whereas, the irreversible one, it can be only reduced by chemical cleaning (Vanysacker *et al*. 2014).

Chemical cleaning is the most common membrane cleaning method, especially in reverse osmosis membranes. It is based on two different mechanisms, chemical and physical interactions. Chemical interactions are related to the reaction between the cleaning agent and the fouling layer. This reaction lowers the structural integrity of the deposited materials, thus facilitates its mechanical removal without damaging the membrane surface by maintaining membrane properties in a safe state. In contrast, physical interactions are related to the mass transport of components from the bulk solution to the membrane surface and from the membrane surface to the bulk solution (Sohrabi *et al*. 2011). Most Cleaning agents are often and commercially available, and many of them are recommended by membrane manufacturers as proprietary chemicals to deal with different types of foulants. They are divided into alkaline and acid cleaners. Acids (nitric, phosphoric, hydrochloric, sulphuric and citric) are often used to remove inorganic scaling, while alkaline ones are suitables for organic fouling removal. Other categories of chemical cleaning agents are metal chelating agents, surfactants and enzymes (Mohammadi *et al*. 2002). The choice of cleaning agents depends mainly on the type of foulants and chemical membrane composition. During the chemical cleaning process, many factors must be considered such as, cleaning agent concentration, system temperature, pH, pressure and cleaning time (Shirazi *et al*. 2010).

In addition, chemical cleaning process can damage the membrane materials and accelerate its ageing process (Simon *et al*. 2013), especially in nanofiltration and reverse osmosis membranes. This problem depends usually on the operating conditions of both the process and the cleaning step. It can result in decline membrane productivity, modification of the membrane properties (membrane hydrophobicity and surface roughness) and alteration of membrane selectivity (Regula *et al*. 2014). As shown in the study performed by Simon *et al*. (2012) to know about the effect of chemical cleaning solutions at different concentrations on a virgin NF270 membranes (Dow Filmtec™), by measuring the membrane zeta potential, hydrophobicity, permeability, and solutes rejection before and after exposure to the cleaning solution during 18 hours at 35°C. Many differences were observed in the membrane characteristics due to membrane ageing; moreover, salt rejection decreased particularly with caustic cleaning and with acidic cleaning at pH below 1.5. On another study focused on the cleaning temperature effect on NF270 membrane ageing, they concluded that the cleaning temperature did not exert any observable impact on the surface charge of the NF270 membrane, but amplified or reduced the impact of the cleaning solution on other membrane properties as well as solute rejection (Simon *et al*. 2013).

On the other hand, chemical cleaning agents had some environmental and economic disadvantages. Environmentally, they cause secondary pollution related to the waste chemical disposal and economically, they add costs of cleanup, handling, transporting dangerous chemicals, waste energy by decreasing and then increasing pressures needed for the membrane system to work, and waste cleaned water (Lu *et al*. 2009). It has been reported that, in general, 5-20% of the operating costs of a large plant are associated with cleaning procedures (Madaeni *et al*. 2001).

As many desalination plants in the world, Sidi Taibi demineralization plant has revealed difficulties related to the membrane performances loss (pressure increase, flux decline, poor quality of the produced water and increase of energy consumption). This behaviour is always a consequence of the fouling phenomenon. In this study an autopsy of a nanofiltration membrane (NF90), that is used in the Sidi Taibi plant, was carried out to determine the origin of the fouling and the nature of the foulants, and three different chemical cleaning solutions (HCl, H_2SO_4 and HNO_3^-, pH 3) were tested and assessed in order to determine the suitable one for the fouled membrane to regain its initial permeability and performances.

2. Materials and methods

2.1 Membrane fouling evaluation

The membrane fouling was evaluated by two methods, non-destructive and destructive methods (membrane autopsy).

2.1.1 Non-destructive method
The monitoring of the permeate flux, pressure, energy consumption and salt rejection as a function of the operating time was carried out continuously during a year of operation at the scale of the Sidi Taibi plant.

Plant description
The establishment of Sidi Taibi plant marked the beginning of the use of a hybrid energy system (photovoltaic and wind) feeding a nanofiltration desalination unit with electrical energy. It was launched in March 2013 at Al Annouar high school of Sidi Taibi, Kenitra, Morocco. The plant was designed to supply the 1200 students of the school with potable water, with a daily production capacity of 12 m^3/day, at a pressure of 5 bar, a recovery rate of 75% and was fed with underground water.

Table 1 Operating characteristics of the membranes used

Parameters	Recommended values	Data source
Maximum Operating Temperature (°C)	45	Manufacturer
Maximum Operating Pressure (bar)	41	Manufacturer
pH Range, Continuous Operation	3 – 10	Manufacturer
Maximum Feed Flow Rate (m³/h)	15.9	Manufacturer
Maximum Feed Silt Density Index (SDI)	5	Manufacturer

Table 2 Characteristics of the raw water and the standards for drinking water fixed by the World Health Organization (WHO)

	Underground water	WHO standards (WHO 2008)
pH	6.79	6.5-8.5
TDS (mg/L)	796.4	500
Na^+ (mg/l)	47	200
NH_4^+ (mg/l)	< 0.1	-
K^+ (mg/l)	11	-
Mg^{2+} (mg/l)	78	50
Ca^{2+} (mg/l)	128	270
F^- (mg/l)	0.04	1.5
Cl^- (mg/l)	57	250
Br^- (mg/l)	< 0.1	-
NO_3^- (mg/l)	68	50
PO_4^{3-} (mg/l)	< 0.1	-
SO_4^{2-} (mg/l)	10	500
Turbidity (NTU)	0.39	5
HCO_3^- (mg/L)	396.53	-
CO_3^{2-} (mg/L)	1.37	-
SDI	< 3	-

The feed water from the underground is pumped into the pilot plant through intake pipes. Firstly, underground water goes to the pre-treatment compartment; it is composed of two cartridges (25µm and 5µm) connected in series, the first one allows the removal of sludge which may be present in the wellbore, it identifies the size of particles less than 25 µm and the second one allows the removal of fine particles greater than 5 µm. Secondly, the pre-treated water is directed into the nanofiltration compartment which consists of two spiral membranes (NF90 40*40) type: polyamide thin-film composite Filmtec Dow, installed in series with a total surface area of 15.2 m² (see Table 1). Thirdly, the nanofiltrated water is routed to be disinfected by an electrochemical disinfection system for the in-situ generation of chlorine. In the final step, the produced water is stored in a storage tank, and distributed.

The fouled nanofiltration membrane element selected for the autopsy study had been in service for nearly one year, from April 2014 to April 2015.

Feed water characterization
The analysis of the raw water (underground water) gives the results shown in table 2.

Experimental methods and Analyses
The Sidi Taibi desalination plant (see Fig. 1) is equipped with different instruments installed at different points in the pilot plant in order to measure all the necessary parameters for this research: pressure, conductivity, flow and temperature.

In addition, the performances of the plant were followed in terms of the salt rejection, permeate flux, recovery rate and the specific energy consumption parameters which are defined as:

- salt rejection (%):

$$R(\%) = \frac{(Gf - Gp)}{Gf} \times 100 \qquad (1)$$

where G_p and G_f are respectively the conductivity of permeate and feed water;

- permeate flux (L/h.m²):

$$Flux = \frac{Qp}{S} \qquad (2)$$

where S (m²) and Qp (L/h) are respectively the surface area of the membrane and permeate flow;

- recovery rate (%):

$$Y = \frac{Qp}{Qf} \times 100 \qquad (3)$$

where Qf and Qp are the feed and the permeate flow rate respectively;

- specific energy consumption (KWh/m³) (Dach 2008, El Harrak *et al*. 2015):

$$E = \frac{\Delta P \times 100}{(\eta \times Y \times 36,6)} \qquad (4)$$

where ΔP, η and Y are the transmembrane pressure (bar), η is the global pumping system efficiency (0.85) and the recovery rate (%), respectively.

2.1.1 Destructive methods (membrane autopsy)
At the laboratory scale, the membrane fouling characterization is completed by following the five steps of membrane autopsy procedure (selection of representative membrane, dissection, analysis, identification and remediation) (Farhat *et al*. 2012). For this reason, analytical techniques are used such as Scanning Electron Microscopy (SEM) connected with an energy dispersive X-ray (EDX) detection system and X-ray diffractometer (XRD) with Cu-Kα1 source with λ= 1,5406 Å.

Fouling evaluation and cleaning processes
Firstly, the membrane for the autopsy is removed from the first stage (see Fig. 1), which faced the majority of fouling problems, and dissected. Secondly the membrane leaves from the outer wrap are detached, and cut for analysis.

Three flat-sheet fouling membranes were implemented from the membrane selected previously and performed at
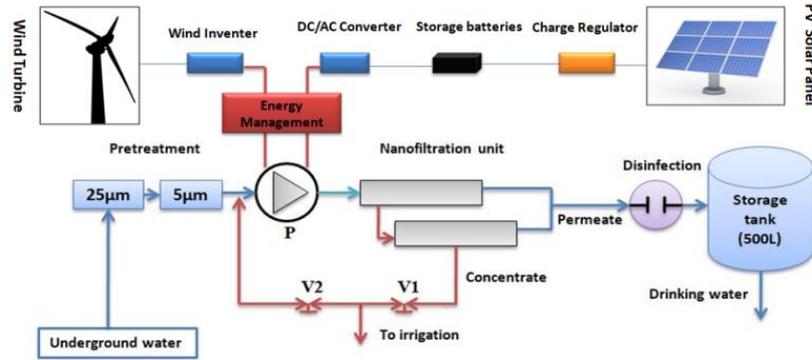
Fig. 1 Operating scheme of the Sidi Taibi desalination plant. V1: Pressure regulation valve; V2: Concentrate recirculation valve; P: High pressure pump
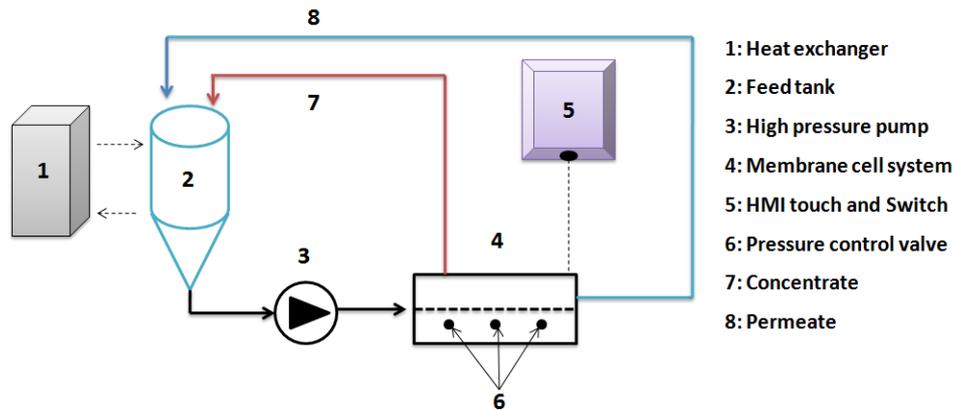

Fig. 2 Schematic diagram of the experimental nanofiltration System used for cleaning tests

the scale of a laboratory pilot cross-flow filtration unit supplied by Sterlitech Corporation (Sterlitech Corporation, WA, USA), equipped with a Sepa CF membrane Cell System (see Fig. 2), with an effective membrane surface area of 140cm^2 for the cleaning tests.

Three different dilute acid solutions are used (HCl (37%), H$_2$SO$_4$ (97%) and HNO$_3^-$ (69%), pH=3) on an alternating circulation (30min) in a single cleaning step preceded and followed by flushing (30min) with a temperature of 23°C and a cleaning pressure of 3bar.

Analytical techniques are used in order to characterize and assess the surfaces of the three cleaned membranes such as a scanning electron microscope (SEM) connected with an energy dispersive X-ray (EDX) detection system.

Chemical cleaning efficiency

To investigate nanofiltration fouling, a virgin nanofiltration membrane (NF90) was used in order to determine the initial membrane water permeability (K (Initial)). After flux stabilization, the initial water permeability was obtained from the slope of normalized permeate flux of distilled water (JN) versus applied pressure (ΔP) at 7; 5.3; 4; 3 and 2 bar. Water temperature was also monitored and permeate flux was normalized to 25°C by means of a correction factor calculated as water viscosity at the temperature of permeation divided by water viscosity at 25°C (Drak *et al.* 2000).

$$K(Initial) = \frac{Qp(\,T°C)}{A \times \Delta P} \times \frac{\mu(T)}{\mu(25\,°C)} = \frac{JN}{\Delta P} \quad (5)$$

where Qp is the permeate flow rate, A is the membrane surface area, $\mu(T)$ is water viscosity at the process temperature, and $\mu(25°C)$ is water viscosity at 25°C.

The fouled membrane water permeability (K_{Fouled}) is obtained after 10 months of operation from the slope of the normalized permeate flux of distilled water versus applied pressure at 7, 6, 5.3, 4, and 3 bar. Finally, the fouled membrane is chemically cleaned, and the membrane water permeability after cleaning procedure ($K_{After\ Cleaning}$) is obtained from the slope of normalized permeate flux of distilled water by applied pressure at 6; 5; 4; 3 and 2 bar.

The membrane cleaning efficiency (MCE) is therefore calculated from three water permeabilities, as shown in Eq. (6) (Sohrabi *et al.* 2011)

$$MCE\ (\%) = \frac{K\ (after\ cleaning) - K\ (fouled)}{K\ (initial) - K\ (fouled)} * 100 \quad (6)$$

where K (after cleaning) is the membrane water permeability after the cleaning procedure, K (fouled) is the fouled membrane water permeability and K (initial) is the initial membrane water permeability.

3. Results and discussion

3.1 Fouling evaluation during NF treatment

Fig. 3 shows the evolution of the permeate flux, pressure, energy consumption and salts rejection versus
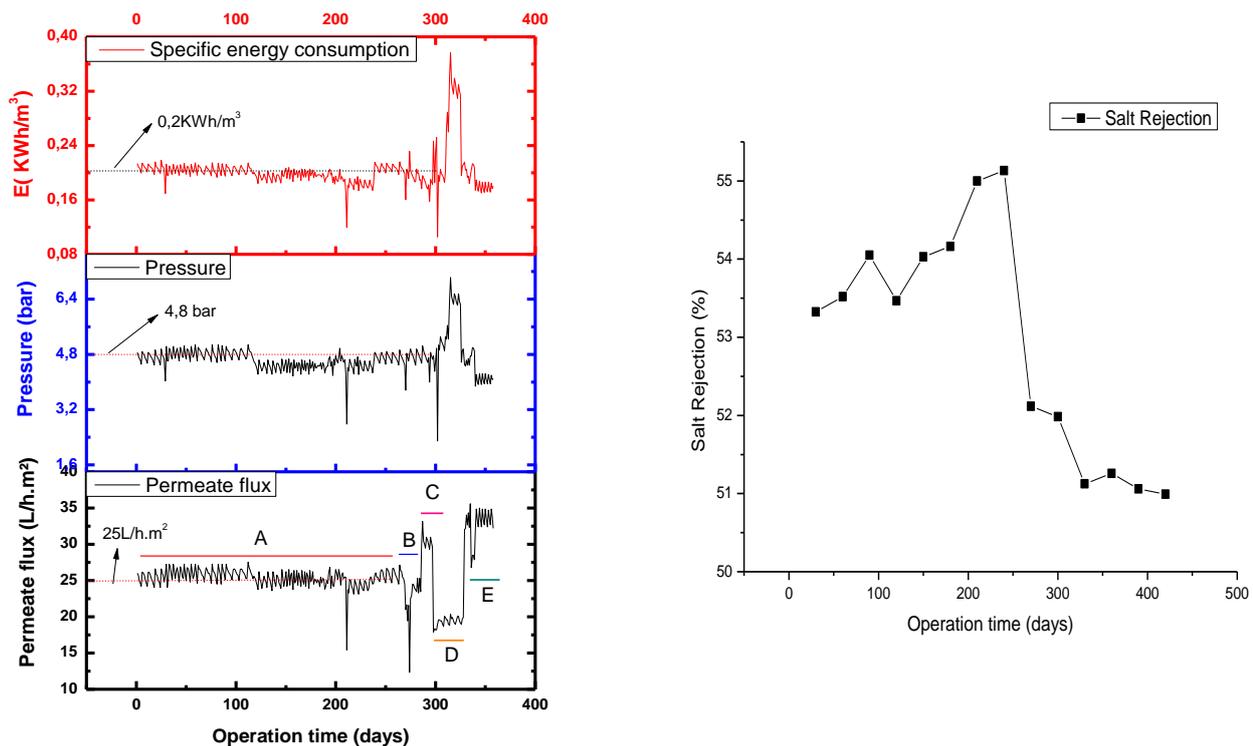
(a) permeate flux, pressure and energy consumption

(b) salt rejection

Fig. 3 Evolution of the permeate flux, pressure, energy consumption and salt rejection vs. time. Period: March 2014 to April 2014

operating time. The monitoring of these parameters makes it possible to evaluate the overall performances of the plant.

In fact, it can clearly be seen that the curves of the permeate flux, pressure and specific energy consumption can be divided into three different zones (see Fig. 3(a)). In the beginning, permeate flux, pressure and specific energy consumption are almost stable around 25L/h.m², 4.8 bar and 0.2KWh/m³, (zone A). This stability is mainly influenced by the compatible execution of the operating parameters of nanofiltration membrane (the pressure: 4.8 bar and the recovery rate 75%), and the operating characteristics of the membranes used in the plant (see table 1). After almost 270 days (9 months) of operation, a slight decrease in permeate flux is observed, which results in a slight increase in the pressure and the energy consumption (zone B). This decreasing of performances can be explained by the beginning of the fouling phenomenon (Qasim *et al.* 2018). As soon as its signs appear, an increase in feed water pressure has been made to ensure a constant permeate flow for a daily needs of potable water (zone C). This operation is done by the frequency regulator of the high-pressure pump which is reflected by an increase in applied feed pressure leading to a higher initial flow. The increase in flow accelerates fouling development (Fernández-Sempere *et al.* 2010). As a results of this phenomenon, permeate flux is gradually declined with 20%, which results in an increase in pressure and specific energy consumption respectively with 22% and 75% (zone D). At the same time, as it is

shown in Fig. 3(b), this membrane has a steady behavior in terms of salt rejection over the operating time. This decreasing of performances is due to problems which require a visual inspection and membrane autopsy in order to identify the nature and origin of the fouling.

In addition, the performances of the plant are improved (zone E) due to the replacement of the first membrane which was sacrificed for the autopsy.

3.2 Characterization of the fouling layer

Generally, the SEM/EDX investigation confirms the variation in the extent of fouling through the membrane surface and also gives further insights into the nature of the fouling layer. As shown in Fig. 4(a), the surface of the fouled membrane include of particulate material covered the entire Nanofiltration membrane surface. This image shows many irregularities at the membrane surface, due to the fouling layer precipitates formed during the treatment, Possibly related to low solubility elements (such as Ca, Mg, Si…) (Shirazi *et al.* 2010, Lin *et al.* 2005). In addition, The EDX analysis indicates that the particulate material had relatively high levels of C (19.29%), O (61.83%) and Ca (18.45%) (see Table 3). Quite low levels of Na, Mg, Al, P, Si, S, and Cl were also present (see Fig. 4(b)) (see Table 3). However, EDX selects a specific area or point to perform the sample analysis (Aguiar *et al.* 2018).

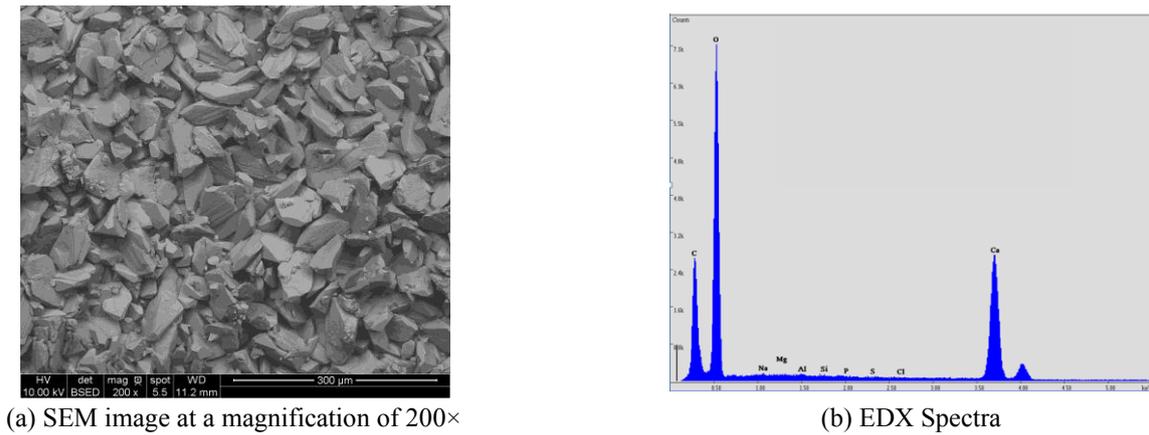The C and O peaks are likely explained by organic

(a) SEM image at a magnification of 200×   (b) EDX Spectra

Fig. 4 SEM image and EDX Spectra of the fouled nanofiltration membrane

Table 3 EDX elemental composition of the fouled nanofiltration membrane

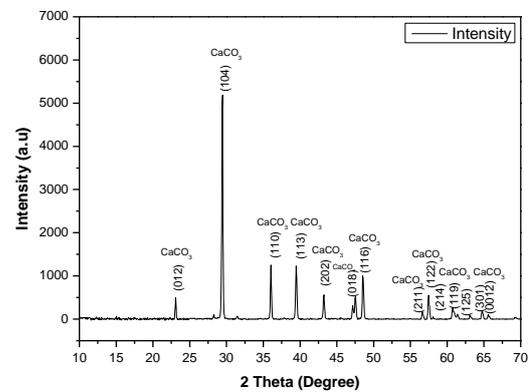| Elements	Atomic %
C	19.29
O	61.83
Na	0.12
Mg	0.05
Al	0.09
Si	0.07
P	0.04
S	0.02
Cl	0.04
Ca	18.45

Fig. 5 X ray of the precipitates found on nanofiltration membrane

and/or biological materials (Salazar-Peláez *et al.* 2017, Zheng *et al.* 2018), which can be due partly to the composition of the polyamide membrane (Sachit and Veenstra 2017), or originated only from the foulant material deposed on the membrane surface, which would indicate that the foulant layers are thicker than the analysis depth of EDX, or maybe from both the foulant layers and the membrane composition (Gorzalski *et al.* 2016). The high peaks of Ca in addition to the high peaks of O and C suggest that the structure of the deposited material is calcium carbonate ($CaCO3$), which is constituent with that observed by many researchers on a thin film composite polyamide membrane surface (Tzotzi *et al.* 2007, Koyuncu and Wiesner\ 2007). Moreover, EDX analysis of the foulant layer showed the presence of S and Cl. The presence of S can be explained by the polysulphone substrate (Zheng *et al.* 2018, Gorzalski *et al.* 2016), whereas Cl ions could have diffused through the polyamide skin layer with some retained in the microporous support (Tran *et al.* 2007).

Furthermore, the presence of Al and Si suggests that it is mainly aluminum silicates, which are common foulants in nanofiltration operations. Given that pre-filters with 25 and 5 µm pore size filters have been used to pre-treat the underground water, the NF feed is likely to be free from larger size silt particles. However, finer particles might remain in the feed and become part of the fouling layer (Salazar-Peláez *et al.* 2017). Hence, Several authors have

studied the chemistry of silica precipitation and they have confirmed the complexity of this phenomenon since it may turn into colloidal silica, calcium silicates or aluminosilicates dependent on feedwater chemistry and system conditions (temperature, pressure…) (Hamrouni and Dhahbi 2001).

Indeed, a range of inorganic compounds are also present in the fouling layer such as Na, Mg and P. These elements can play an essential role in the formation and the density of foulants, because they can link the deposited cells and bio-polymers previously deposited on the membrane and then formed a dense cake layer when passing through the membranes (An *et al.* 2009). Besides, they could lead not only to an inorganic crystallization by acting as a heterogeneous epitaxic sites but also precipitate at specific sites into the extracellular polymeric substances and producing biominerals at the membrane surface by organic and inorganic interactions (Herrera-Robledo *et al.* 2011).

X-ray diffraction is also used to characterize foulants on the membrane surface. The XRD patterns are displayed in Fig. 5, all the diffraction peaks can be exclusively attributed to $CaCO_3$ with a rhombohedral structure without any other secondary phases.

The average grain size is calculated by using Debye-Scherrer equation ($G = 0.9 \times \lambda / \beta \times \cos(\theta)$), where λ, θ and β are the X-ray wavelength (Cu, 1.5418 Å), the maximum of
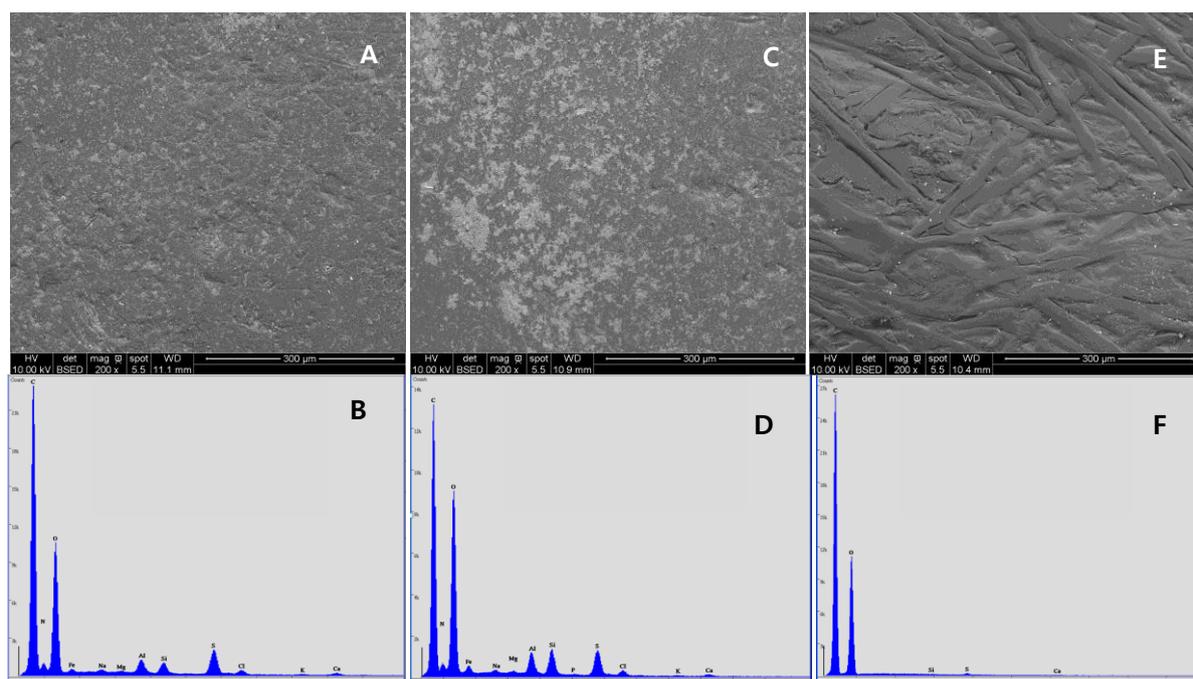
Fig. 6 SEM images at a magnification of 200× and EDX spectra of membrane surfaces after cleaning procedure (A, B) Sulfuric Acid cleaning; (C, D) Nitric Acid cleaning; (E, F) Hydrochloric Acid cleaning

the Bragg diffraction peak, and the full width at half maximum, respectively. The average value obtained for the crystallites is 48 nm; this value is calculated after an instrumental broadening correction.

Finally, The SEM images, EDX spectra and X-ray diffraction suggest that the fouled material is mainly inorganic matter, and the major crystal deposited on the NF membrane is calcium carbonate ($CaCO_3$).

3.3 Evaluation of membrane cleaning

3.3.1 Visual evaluation and elemental composition of cleaned membrane samples (SEM/EDX)

Initially, three samples of flat sheet fouling membranes are cleaned with three different solutions of dilute acid (HCl, H_2SO_4 and HNO_3^-, pH 3) and imaged by SEM and the corresponding EDX spectra to reveal the morphology of the cleaned membrane surfaces and also to compare them to the fouled membrane surface (previously characterized).

Figure 6 demonstrates the extent of scale formation at a magnification of 200× and EDX spectra, across the three studied cleaned membrane surfaces: H_2SO_4 (see Figs 6 (A)-(B)), HNO_3^- (see Figs 6 (C)-(D)), HCl (see Figs 6 (E)-(F)).

According to Fig. 6 (A), the layer of the fouling material from the cleaned membrane with sulfuric acid is almost covering the entire surface of the membrane. In addition, the layer of the fouled material from the cleaned membrane with nitric acid has partially covered the surface of the membrane with a few irregularities (see Fig.6 (C)). These irregularities become even less visible after the membrane has been cleaned with hydrochloric acid (see fig.6 (E)). Moreover, the obtained results from EDX demonstrated show the effectiveness of the three cleaning acids proposed for the autopsied membrane. Based on these results, the
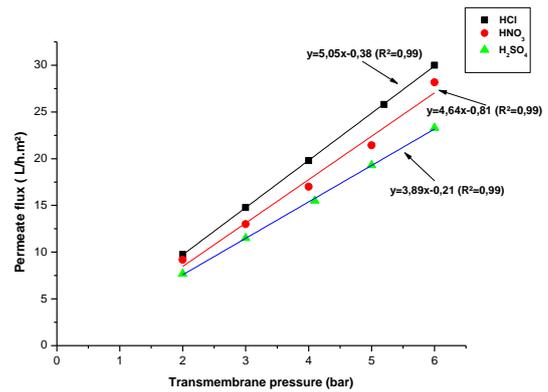
Table 4 EDX elemental composition of the three samples of flat sheet fouling membrane after acids cleaning

Element	Atomic %		
	Sulfuric acid	Nitric acid	Hydrochloric acid
C	62.38	56.63	66.08
N	6.76	6.28	33.62
O	25.20	29.69	-
Fe	0.65	1.31	-
Na	0.16	0.19	-
Mg	0.08	0.10	-
Al	0.87	1.20	-
Si	0.80	1.65	0.02
P	-	0.03	-
S	2.23	2.07	0.21
Cl	0.42	0.46	-
K	0.10	0.10	-
Ca	0.33	0.21	0.08

amounts of inorganic compounds such as silica, aluminum, magnesium, iron, sodium, chloride and potassium on the membrane surface after chemical cleaning with sulfuric acid have been very negligible and very close to the amount of these inorganics on the membrane surface after nitric acid cleaning (see figs.6 (B)-(D)). Furthermore, both spectra show that the precipitated calcium level on the surfaces of the two cleaned membranes decreases from 0.33% (sulfuric acid) to 0.21% (nitric acid) (see Table 4). In addition, fig.6 (F) and table 4 show slight levels of calcium (0.08%) and silica (0.02%), and no others inorganic compounds are
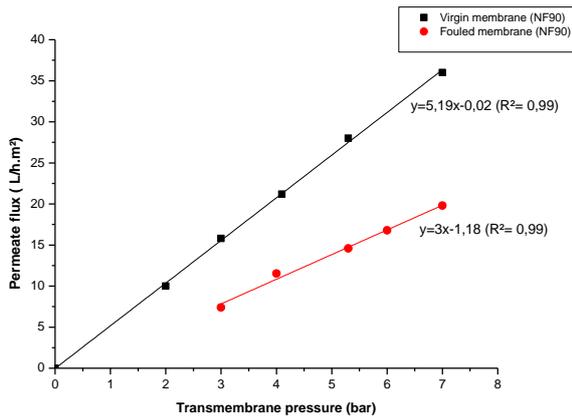
(a)   Virgin and fouled membranes   (b)   Cleaned membranes

Fig. 7 NF90 membrane water permeability of virgin, fouled and cleaned membranes with Hydrochloric Acid, Nitric Acid and Sulfuric Acid

Table 5 Water permeabilities of virgin membrane, fouled membrane, cleaned membranes and the cleaning efficiency of the three acids (HCl, H_2SO_4 and HNO_3^-)

	L_p^* ($L.h^{-1}.m^{-2}.bar^{-1}$)	MCE^* (%)
Virgin membrane (NF90)	5.19	-
Fouled membrane (NF90)	3	-
Fouled membrane after hydrochloric acid cleaning	5.05	93%
Fouled membrane after sulfuric acid cleaning	3.89	40%
Fouled membrane after nitric acid cleaning	4.64	74%

*L_p: Water permeability; *MCE: Membrane cleaning efficiency

detected on the membrane surface after hydrochloric acid cleaning. Likewise, the three spectra (see figs.6 (B)-(D)-(F)) show a high level of carbone and oxygen in the deposited material of the three cleaned membranes.

A further observation is the detection of nitrogen in the surface of the cleaned membrane by sulfuric acid and nitric acid, in contrast to the membrane surface cleaned by hydrochloric acid; it's probably due to the analysis depth of EDX (Gorzalski *et al.* 2016).

Based on what has been mentioned in this section, it's clear that the chemical cleaning with hydrochloric acid is remarkably effective to remove inorganic foulants from the autopsied membrane surface.

3.3.2 Chemical cleaning efficiency

Figure 7 (a) shows the membrane water permeability of virgin membrane ($K_{initial}$) and fouled membrane (K_{fouled}), and Figure 7 (b) shows also the membrane water permeability after cleaning procedure with hydrochloric acid, sulfuric acid and nitric acid. According to these results, after nearly ten months of operation, the membrane water permeability decreases by 41 %, due to membrane fouling.

The main foulants on the surface of the previously autopsied membrane are inorganic salts, and more precisely calcium carbonate scale.

The permeabilities of the three fouling membrane samples, after acids cleaning, are determined and results indicate in Table 5.

Based on these results (see Table 5), the membrane water permeability is improved thanks to the three studied acids cleaning, particularly with hydrochloric Acid. These results are in concordance with decreasing of roughness membrane surface after hydrochloric acid cleaning as shown by SEM and EDX (see Fig. 6).

This study focuses on acidic cleaning solutions because they are more efficient for inorganic foulants due to the low structural integrity of the fouling layer upon the reaction of the membrane foulants with the acid solution (Goh *et al.* 2018). In addition, other study reported an increase in permeate conductivity after membrane cleaning with an alkaline solution ((NaOH) at pH 11) and as well as an increase in permeate conductivity for acidic solutions, especially, citric acid only at a pH as low as 1.5 (Simon *et al.* 2013).

Among the evaluated acidic cleaning solutions, sulfuric acid showed the lowest cleaning efficiency. This can be explained by the increase of sulfate concentrations on the membrane surface that can lead to the formation of salts with low solubility in the presence of cations such as Calcium and Magnesium ions (Shirazi *et al.* 2010). The highest cleaning efficiency is obtained with hydrochloric acid (93%) and nitric acid (74%) (see Table 5).

The price per cleaning agent mass is a principal factor to choose the best cleaning acid. Furthermore, a previous study (Aguiar *et al.* 2018) report that the lowest prices per cleaning agent mass were obtained by nitric acid and sulfuric acid in comparison with hydrochloric acid for the NF270 after gold Acid mine drainage treatment. Yet, the low cleaning efficiency of sulfuric acid and the possibility of the salts formed with sulfate discourage its use as a membrane-cleaning agent (Xie *et al.* 2004).

Hence, the cleaning efficiency of hydrochloric acid (93%) is higher than that of nitric Acid (74%), it is chosen as the best chemical cleaning agent for the nanofiltration

(NF90) membrane after underground water treatment.

4. Conclusions

This paper presents the autopsy results of a nanofiltration membrane after nearly 10 months of operation. The sample of the fouled membrane was analyzed by Scanning Electron Microscopy (SEM) connected with an energy dispersive X-ray (EDX) detection system and X-ray diffractometer (XRD) in order to provide us about foulants composition and the adequate solutions to solve it.

The results obtained are complementary and reveal the problems caused by the accumulation of deposits on the membrane surface. The most prominent conclusions are the following:
- Sodium, Magnesium, Aluminum, Silicate and calcium are the main inorganics elements found on the membrane surface;
- SEM images, EDX spectra and X-ray diffraction suggest that the fouled material is inorganic consisting mainly of calcium carbonate;
- Membrane fouling is responsible for a decrease in water permeability by 41% and could be partially removed by chemical cleaning;
- Permeability is improved by the hydrochloric acid cleaning (pH=3) with a cleaning efficiency of 93%. Furthermore, cleaning efficiency did not exceed 75 % with nitric acid (pH=3) and 40 % with sulfuric acid (pH= 3).

The results are discussed on the basis of recent studies related to the new trends in conception. The following recommendations can be proposed:
- Regular maintenance of pre-filters in order to avoid the flight of sand particles;
- Use an efficient antiscalant in order to prevent precipitations of salts, particularly calcium carbonate;
- Clean membranes when performances of the plant are declined. The cleaning solution proposed according to the foulant is: hydrochloric acid (pH 3) preceded and followed by flushing.

References

Abid, H. S., Johnson, D. J., Hashaikeh, R. and Hilal, N. (2017), "A review of efforts to reduce membrane fouling by control of feed spacer characteristics", *Desalination*, **420**, 384-402. https://doi.org/10.1016/j.desal.2017.07.019.

Aguiar, A., Andrade, L., Grossi, L., Pires, W. and Amaral, M. (2018), "Acid mine drainage treatment by nanofiltration: A study of membrane fouling, chemical cleaning, and membrane ageing", *Separation Purification Technol.*, **192**, 185-195, https://doi.org/10.1016/j.seppur.2017.09.043.

An, y., Wang, Z., Wu Z., Yang, D. and Zhou, Q. (2009), "Characterization of membrane foulants in an anaerobic nonwoven fabric membrane bioreactor for municipal wastewater treatment", *Chem. Eng. J*, **155**(3), 709-715. https://doi.org/10.1016/j.cej.2009.09.003.

Dach, H. (2008), "Comparison of the operations of nanofiltration and reverse osmosis for the selective desalination of brackish water: of the scale of the laboratory to the industrial pilot", Ph.D. Dissertation, Université d'Angers, France.

Drak, A., Glucina, K., Busch, M., Hasson, D., Laîne, J.M. and Semiat, R. (2000), "Laboratory technique for predicting the scaling propensity of RO feed waters", *Desalination*, **132**(1-3), 233-242. https://doi.org/10.1016/S0011-9164(00)00154-5.

El Harrak, N., Elazhar, F., Belhamidi, S., Elazhar, M., Touir, J., and Elmidaoui, A. (2015), "Comparaison des performances des deux procédés membranaires: la Nanofiltration et de l'Osmose inverse dans le Dessalement des eaux saumâtres (Performances comparison of two membranes processes: Nanofiltration and Reverse Osmosis in brackish water Desalination)", *J. Mater. Environ. Sci*, **6**(2), 383-390

Epsztein, R., Cheng, W., Shaulskya, E., Dizge, N. and Elimelech, M. (2018), "Elucidating the mechanisms underlying the difference between chloride and nitrate rejection in Nanofiltration", *J. Membrane Sci.*, **548**(15), 694-701. https://doi.org/10.1016/j.memsci.2017.10.049.

Epsztein, R., Nir, O., Lahav, Ori. and Green, M. (2015), "Selective nitrate removal from groundwater using a hybrid nanofiltration–reverse osmosis filtration scheme", *Chem. Eng. J.*, **279**, 372-378. https://doi.org/10.1016/j.cej.2015.05.010.

Fang, L.F., Zhou, M.Y., Cheng, L., Zhu, B.K., Matsuyama, H. and Zhao, S. (2019), "Positively charged Nanofiltration membrane based on cross-linked polyvinyl chloride copolymer", *J. Membr. Sci.*, **527**, 28-37. https://doi.org/10.1016/j.memsci.2018.10.054.

Farhat, S., Kamel, F., Jedoui, Y. and Kallel, M. (2012), "The relation between the RO fouling membrane and the feed water quality and the pretreatment in Djerba Island plant", *Desalination*, **286**, 412-416. https://doi.org/10.1016/j.desal.2011.11.058.

Fernández-Sempere, J., Ruiz-Beviá, F., García-Algado, P. and Salcedo-Díaz, R. (2010), "Experimental study of concentration polarization in a crossflow reverse osmosis system using Digital Holographic Interferometry", *Desalination*, **257**(1-3), 36-45. https://doi.org/10.1016/j.desal.2010.03.010.

Goh, P.S., Lau, W.J., Othman, M.H.D. and Ismail, A.F. (2018), "Membrane fouling in desalination and its mitigation strategies", *Desalination*, **425**, 130-155. https://doi.org/10.1016/j.desal.2017.10.018.

Gorzalski, A.S., Donley, C. and Coronell, O. (2016), "Elemental composition of membrane foulant layers using EDS, XPS, and RBS", *J. Membr. Sci.*, **522**(15), 31-44. https://doi.org/10.1016/j.memsci.2016.08.055.

Hamrouni, B. and Dhahbi, M. (2001), "Analytical aspects of silica in saline water - Application to desalination of brackish waters", *Desalination*, **136**, 225-232. https://doi.org/10.1016/S0011-9164(01)00185-0.

Herrera-Robledo, M., Cid-León, D.M., Morgan-Sagastume, J.M. and Noyola, A. (2011), "Biofouling in an anaerobic membrane bioreactor treating municipal sewage", *Sep. Purif. Technol*, **81**(1), 49-55. https://doi.org/10.1016/j.seppur.2011.06.041.

Jadhav, S.V., Marathe, K.V. and Rathod, V.K. (2016), "A pilot scale concurrent removal of fluoride, arsenic, sulfate and nitrate by using nanofiltration: Competing ion interaction and modelling approach", *J. Water Process Eng.*, **12**, 153-167. https://doi.org/10.1016/j.jwpe.2016.04.008.

Jiang, S., Li, Y. and Ladewig, B.P. (2017) "A review of reverse

osmosis membrane fouling and control strategies", *Sci. Total Environ.*, **595**, 567-583. https://doi.org/10.1016/j.scitotenv.2017.03.235.

Karime, M., Bouguechab, S. and Hamrounia, B. (2008), "RO membrane autopsy of Zarzis brackish water desalination plant", *Desalination*, **220**, 258-266. https://doi.org/10.1016/j.desal.2007.02.040.

Kimura, K., Hane, Y., Watanab, Y., Amy, G. and Ohkuma, N. (2004), "Irreversible membrane fouling during ultrafiltration of surface water", *Water Res.*, **38**(14-15), 3431-3441. https://doi.org/10.1016/j.watres.2004.05.007.

Koyuncu, I. and Wiesner, M.R. (2007), "Morphological variations of precipitated salts on NF and RO membranes", *Environ. Eng. Sci.* **24**, 602-614. https://doi.org/10.1016/j.watres.2004.05.007.

Lee, D.J., Lin, J.C.T. and Huang, C. (2010), "Membrane fouling mitigation: Membrane cleaning", *Separation Science and Technology*, **45**, 858-872. https://doi.org/10.1080/01496391003666940.

Leo, C.P., Yeo, K.L., Lease, Y. and Derek, C.J.C. (2016), "Fouling evaluation on nanofiltration for concentrating phenolic and flavonoid compounds in propolis extract", *Membr. Water Treat.,* **7**(4), 327-339. https://doi.org/10.12989/mwt.2016.7.4.327.

Lin, C. J., Shirazi, S. and Rao, P. (2005), "Mechanistic model for CaSO4 fouling on Nanofiltration membrane", *J. Environ. Eng.*, **131**(10), 1387-1392.

Lu, J.Y., Du, X. and Lipscomb, G. (2009), "Cleaning membranes with focused ultrasound beams for drinking water treatment", *Proceedings of IEEE International Ultrasonics Symposium Proceedings*, 1195-1198, Roma, Italy, September.

Madaeni, S.S., Mohamamdi, T. and Moghadam, M.K. (2001), "Chemical cleaning of reverse osmosis membranes", *Desalination*, **134** (1-3), 77-82. https://doi.org/10.1016/S0011-9164(01)00117-5.

Mohammadi, T., Madaeni, S.S. and Moghadam, M.K. (2002), "Investigation of membrane fouling", *Desalination*, **153** (1-3), 155-160. https://doi.org/10.1016/S0011-9164(02)01118-9.

Pontié, M., Dach, H., Leparc, J., Hafsi, M. and Lhassani, A. (2008), "Novel approach combining physico-chemical characterizations and mass transfer modelling of nanofiltration and low pressure reverse osmosis membranes for brackish water desalination intensification", *Desalination*, **221**, 174-191. https://doi.org/10.1016/j.desal.2007.01.075.

Qasim, M., Darwish, N. N., Mhiyo, S., Darwish, N.A. and Hilal, N. (2018), "The use of ultrasound to mitigate membrane fouling in desalination and water treatment", *Desalination*, **443**, 143-164. https://doi.org/10.1016/j.desal.2018.04.007.

Regula, C., Carretier, E., Wyart, Y., Gésan-Guiziou, G., Vincent, A., Boudot, D. and Moulin, P. (2014), "Chemical cleaning/disinfection and ageing of organic UF membranes: A review", *Water Res*, **56**, 325-365. https://doi.org/10.1016/j.watres.2014.02.050.

Ruiz-Garcíaa, A., Melián-Martelb, N. and Mena, V. (2018), "Fouling characterization of RO membranes after 11 years of operation in a brackish water desalination plant", *Desalination*, **430**, 180-185. https://doi.org/10.1016/j.desal.2017.12.046.

Sachit, D. E. and Veenstra J. N. (2017), "Foulant analysis of three RO membranes used in treating simulated brackish water of the Iraqi marshes", *Membranes (Basel)*, **7**(2), 23. https://doi.org/10.3390/membranes7020023.

Salazar-Peláez, M.L., Morgan-Sagastume, J.M. and Noyola, A. (2017), "Fouling layer characterization and pore-blocking mechanisms in an UF membrane externally coupled to a UASB reactor", *Water SA*, **43**(4), 573-580. http://dx.doi.org/10.4314/wsa.v43i4.05.

Shirazi, S., Lin, C. and Chen, D. (2010), "Inorganic fouling of pressure-driven membrane processes-A critical review", *Desalination*, **250**, 236-248.

https://doi.org/10.1016/j.desal.2009.02.056.

Simon, A.R., Price, W.E. and Nghiem, L.D. (2012), "Effects of chemical cleaning on the nanofiltration of pharmaceutically active compounds (PhACs)", *Separation Purification Technol.*, **88**, 208-215. https://doi.org/10.1016/j.seppur.2011.12.009.

Simon, A., Price, W.E. and Nghiem, L.D. (2013), "Impact of chemical cleaning on the nanofiltration of pharmaceutically active compounds (PhACs): the role of cleaning temperature", *J. Taiwan Inst. Chem. Eng.*, **44**(5), 713-723. https://doi.org/10.1016/j.jtice.2013.01.030.

Sohrabi, M.R., Madaeni, S.S., Khosravi, M. and Ghaedi. A.M. (2011), "Chemical cleaning of reverse osmosis and nanofiltration membranes fouled by licorice aqueous solutions", *Desalination*, **267**(1), 93-100. https://doi.org/10.1016/j.desal.2010.09.011.

Song, Y., Li, T., Zhou, J., Li, Z. and Gao, C. (2016), "Analysis of nanofiltration membrane performance during softening process of simulated brackish groundwater", *Desalination*, **399**, 159-164. https://doi.org/10.1016/j.desal.2016.09.004.

Tarek, S.J., Ahmad, M.S., Eman, S.M., Ahmed, A.K. and Azza, M.A.E.A. (2018), "Application of nanofiltration membrane for the River Nile water treatment in Egypt: Case study", *Membr. Water Treat.*, **9**(4), 233-243. http://dx.doi.org/10.12989/mwt.2018.9.4.233.

Tran, T., Bolto, B., Gray, S., Hoang, M. and Eddy, O. (2007), "An autopsy study of a fouled reverse osmosis membrane element used in a brackish water treatment plant", *Water Res.*, **41**, 3915-3923. https://doi.org/10.1016/j.watres.2007.06.008.

Tzotzi, C., Pahiadaki, T., Yiantsios, S.G., Karabelas, A.J. and Andritsos, N.A. (2007), "Study of CaCO3 scale formation and inhibition in RO and NF membrane processes", *J. Membr. Sci*, **296**, 171-184. https://doi.org/10.1016/j.memsci.2007.03.031.

Vanysacker, L., Bernshtein, R. and Vankelecom, I.F.J. (2014), "Effect of chemical cleaning and membrane aging on membrane biofouling using model organisms with increasing complexity", *J. Memb. Sci*, **457**, 19-28. https://doi.org/10.1016/j.memsci.2014.01.015.

World Health Organization (2008), *Guidelines for Drinking-Water Quality: Incorporating 1st and 2nd Addenda, Vol. 1, Recommendations*, 375-492.

Xie, R.J., Gomez, M.J., Xing, Y.J. and Klose, P.S. (2004), "Fouling assessment in a municipal water reclamation reverse osmosis system as related to concentration factor", *J. Environ. Eng. Sci.*, **3**, 61-72. https://doi.org/10.1139/s03-054.

Zheng, L., Yu, D., Wang, G., Yue, Z., Zhang, C., Wang, Y., Zhang, J., Wang, J., Liang, G. and Wei, Y. (2018), "Characteristics and formation mechanism of membrane fouling in a full scale RO wastewater reclamation process: Membrane autopsy and fouling characterization", *J. Membr. Sci.*, **563**(1), 843-856. https://doi.org/10.1016/j.memsci.2018.06.043.

CC